Particle Correlations in Proton-Nucleon Collisions at 205 GeV/c

G. Fujioka, H. Fukushima, M. Igarashi, K. Kobayakawa, M. Miyagaki, T. Morii, Y. Tsuzuki, H. Yamasaki, S. Konishi*, O. Kusumoto*, H. Okabe* S. Ozaki*, M. Teranaka*, M. Ohta**, J. Yokota+, K. Kitayama++

Department of Physics, Kobe University, Kobe.
* Department of Physics, Osaka City University, Osaka.
** Department of Physics, Kinki University, Higashi-Osaka.
\+ Science Education Institute of Osaka Prefecture, Osaka.
++ Department of Physics, Wakayama Medical College, Wakayama.

A study on particle correlations was done by scanning a stack of nuclear emulsion exposed to the 205 GeV/c proton beam at FNAL. The 307 events of $0 + n_s$ are selected to be analyzed. Among them 150 events have slow electrons (mostly one) and/or a track of its length less than 3 μm (dirty event). The rest without such a track is the clean evnt which are considered to be proton-nucleon collisions.

The correlations of prongs in their rapidities and emitted angles (θ, ϕ) are investigated for different multiplicities, even and odd, small and large multiplicities. No significant difference in the distributions of correlation quantities is found between in clean and dirty events and also in even (p - p) and odd (p - n) multiplicity events. The short range and long range correlations are discussed by considering independent emission from inclusive distribution.

1. The two particle correlations are studied by analyzing an emulsion stack exposed to the 205 GeV/c proton beam at FNAL. Along-the-track scanning was performed over the total length 1060 m and 2963 inelastic events were detected. Among them, there were 436 events without heavily ionizing track which are considered as proton-nucleon collisions. Measurements on the emitted angle of each track with an accuracy around 10^{-4} rad were done for $0 + n_s$. The present data are from a sample of 307 events except $n_s = 1$ and coherent type[1] with $n_s = 3,5$ and 7. The latter are excluded under the condition $\Sigma m_i \sin\theta_\ell(i) < 0.06$ GeV where m_i and $\theta_\ell(i)$ are the mass and the emitted angle in ℓs of i-th outgoing particle[1].

2. As a step beyond the study of inclusive particle distribution, two particle correlation studies are widely investigated[2]. Still intensive studies from various standpoint seems to be necessary. In this paper we study the correlations in rapidity, azimuthal angle and emitted angle in cms. 307 $0 + n_s$ events above mentioned are firstly divided into dirty (D) events which have one or more electrons and/or a track of its length less than and 3μm and clean (C) events which have no such a prong. Events are then classified to small ($n_s \leq 11$) and large ($n_s \geq 12$) multiplicities and also even and odd prongs. The number of prongs in each class is shown in Table I. The average multiplicities for clean and dirty are also shown and are a little bit more than hydrogen bubble chamber data.

TABLE I

p + EMULSION AT 205 Gev/c

$0 + n_s$ EVENTS EXCEPT COHERENT TYPE

CLEAN 157 EV. $\langle n_s \rangle = 8.83 \pm 0.71$

CLASS	No. of Pr.	No. of Comb.
SMALL ($n_s \leq 11$)	871	3057
LARGE ($n_s \geq 12$)	516	3603
EVEN	750	3547
ODD	637	3113

DIRTY (e AND/OR RECOIL) 150 EV. $\langle n_s \rangle = 9.05 \pm 0.74$

CLASS	No. of Pr.	No. of Comb.
SMALL ($n_s \leq 11$)	827	2992
LARGE ($n_s \geq 12$)	531	4052
EVEN	496	2908
ODD	862	4136

cf. B.C. $\langle n_s \rangle = 7.68 \pm 0.07$

Since the momentum is not measured in our case, the rapidity is here defined by

$$Y_\ell(i) = -\log\tan(\theta_\ell(i)/2), \qquad (1)$$

$$Y_{cm}(i) = Y_\ell(i) - \log(\gamma_c + \sqrt{\gamma_c^2 - 1}) - \log B, \qquad (2)$$

and the emitted angle, θ^*, in cms is estimated by

$$\tan(\theta^*(i)/2) = \gamma_c B \tan\theta_\ell(i), \qquad (3)$$

where γ_c is the Lorentz factor of cms and B is a correction factor for transverse momentum such as $B = \langle (P_t^2 + \mu^2)^{1/2}/P_t \rangle$; γ_c, B are 10.48 and 1.37 respectively in our case.

To see the correlation, three quantities, $\Delta\phi$, Δy and $\cos\theta^*_{ij}$ defined below are calculated for every combination of prongs for each event.

$$\Delta y = y_{cm}(i) - y_{cm}(j) = y_\ell(i) - y_\ell(j), \; Y_\ell(i) > Y_\ell(j), \qquad (4)$$

$$\Delta\phi = \phi(i) - \phi(j), \qquad (5)$$

and $\cos\theta^*_{ij}$ is the direct cosine between two prongs in cms. The total number of the combination in each class is listed in Table I.

3. The distributions of the azimuthal correlation, $\Delta\phi$ are shown for the classes of small, large, even and odd of C-events in Fig. 1 (a), (b), (c) and (d), respectively. All distributions as well as those for D-events (not shown) are almost uniform which means no correlation. However, for clean small events there is a small tendency of anticorrelation. In this case, if we select $\Delta\phi$ for small Δy, say, < 0.8, this anticorrelation is enhanced. This shows that there is a tendency to form a low mass clusterization.

4. The inclusive y_{cm} distributions for C-events are presented in Fig. 2. The dispersions, $\sigma(Y)$ are calculated. The histogram are well represented by Gaussian curves (solid curves) with $\sigma(Y)$. The distribution of small case is clearly broader than that of large case. This may be due to the effect of diffraction type mechanism. The similar distributions are obtained in D-events.

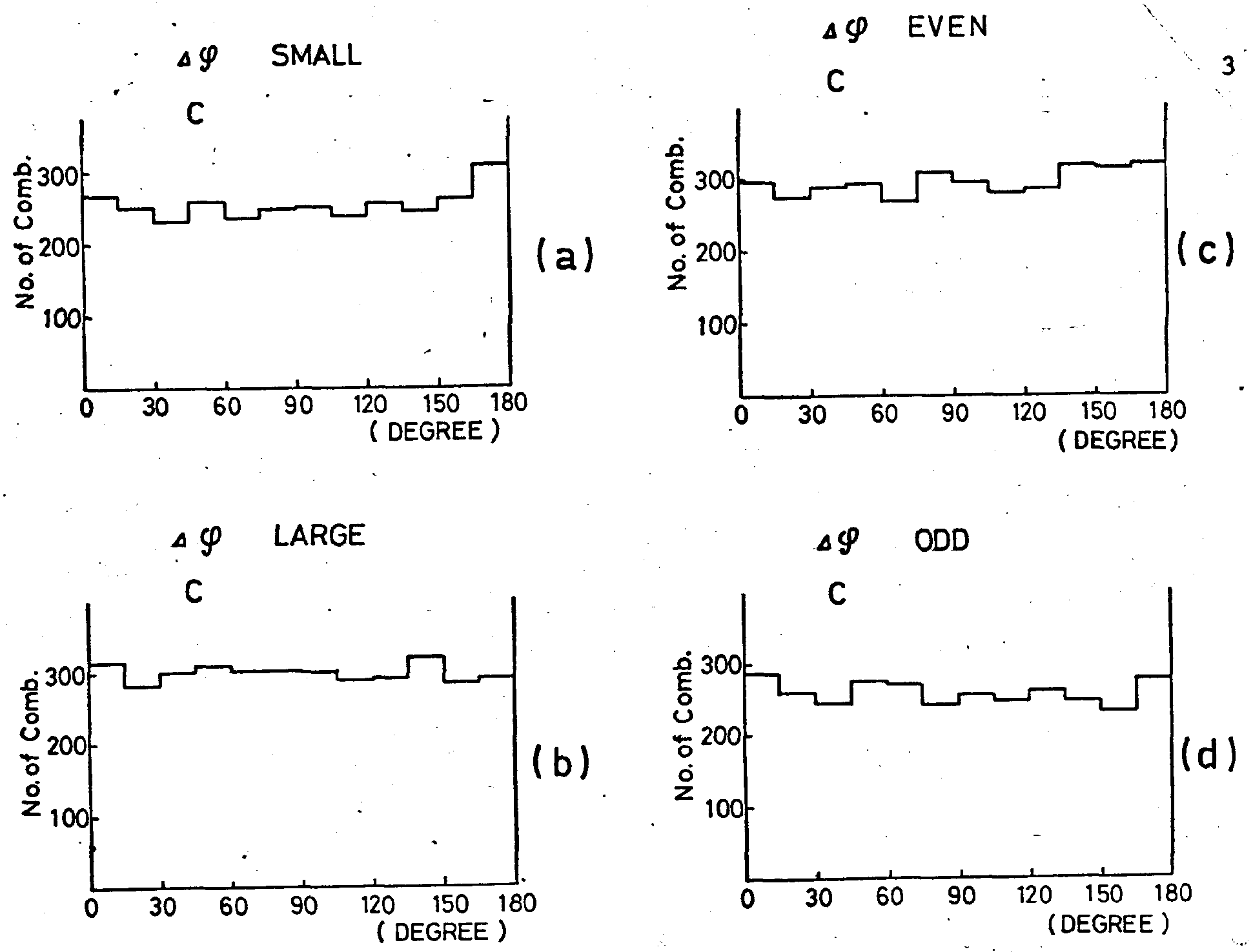

Fig. 1 Correlation of $\Delta\phi$ for C-events.

To make the correlation in Y clear, the following procedure is performed. If the particle are emitted independently under the inclusive Y-distribution which is the Gaussian curve with $\sigma(Y)$, then the ΔY distribution becomes the Gaussian curve with dispersion $\sqrt{2}\sigma(Y)$. This no correlated curve can be compared with experimental histogram as shown in Fig. 3.
In Table II, $\sigma(Y)$, $\sqrt{2}\sigma(Y)$ and $\sigma(\Delta Y)$ for all cases are listed. As can be seen, $\sigma(\Delta y)$ is lower than $\sqrt{2}\sigma(Y)$ in each case. Fig. 3 shows that the main difference between ΔY distribution and the no correlated curve comes from small Δy region where the data exceed than the curve beyond the statistical error. The difference in small case is significant than that in large case.
In the large Δy region there are no significant difference between the data and the curve as shown in the side of Fig. 3. It can be said that some short-range correlation exist and the long-range correlation is not remarkable. The similar distributions of Y_{cm} and ΔY are obtained in even and odd cases.

5. In Fig. 4 the inclusive $\cos\theta^*$ distributions for C small and for C large cases are shown. In small case, the distribution has the sharper peaks at $\eta = \cos\theta^* = \pm 1$ than that in large case. This is essentially same with that $\sigma(Y)$ for the former case is larger than $\sigma(Y)$ for the latter case.

To see the angular correlation, at first, the experimental η-distribution is assumed to be expressed in the form of $f(\eta) = \Sigma_{n=0}^{3} a_n \eta^{2n}$. If particles distribute uniformly in ϕ and haye no correlation, then we expect $Z(= \cos\theta^*_{ij})$ distribution such as

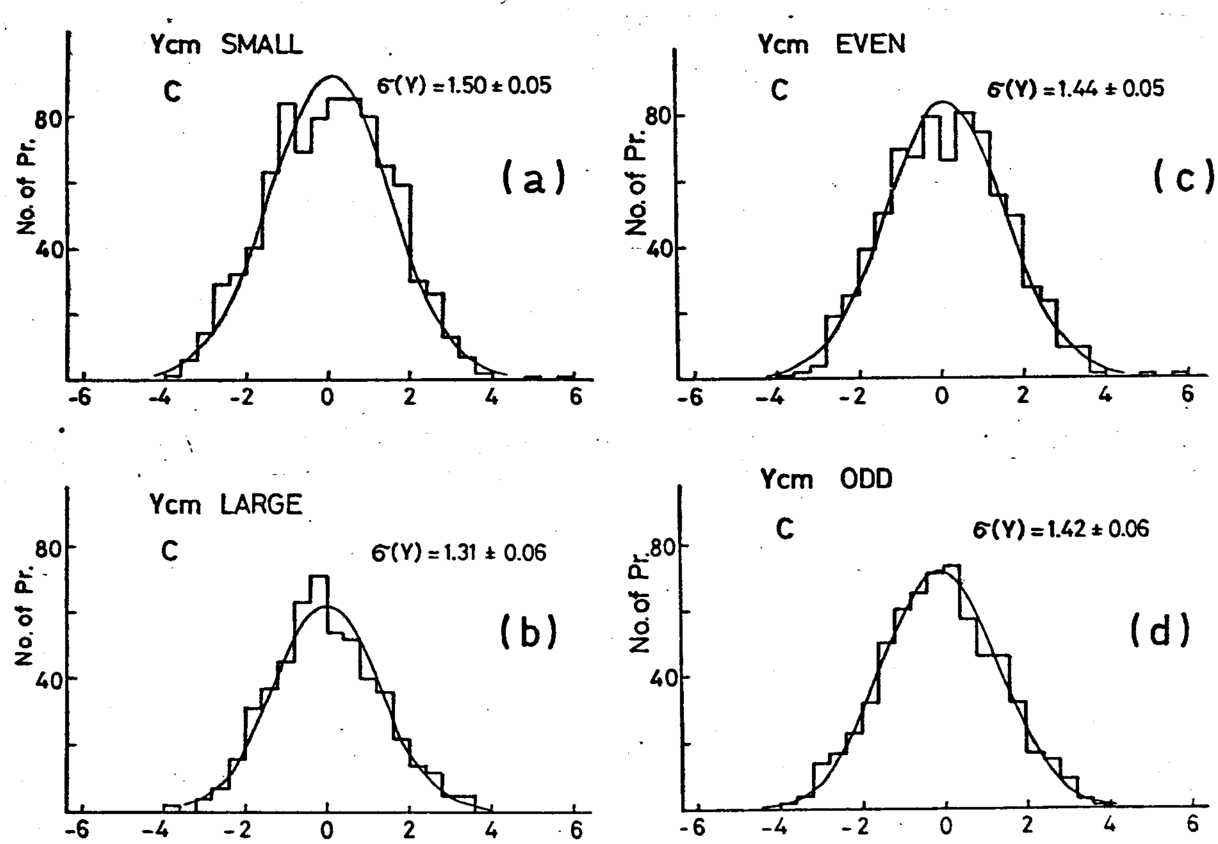

Fig. 2 Inclusive distribution of Y_{cm} for C-events. The solid line is Gaussian curve with σ(Y).

TABLE II

Ycm, ΔY — DISTRIBUTION

		σ(Y)	√2 σ(Y)	σ(ΔY)
C	SMALL	1.502 ± .051	2.124 ± .072	2.073 ± .037
	LARGE	1.313 ± .058	1.856 ± .082	1.802 ± .030
	EVEN	1.437 ± .052	2.032 ± .074	1.934 ± .032
	ODD	1.422 ± .056	2.011 ± .080	1.928 ± .035
D	SMALL	1.463 ± .051	2.069 ± .072	1.942 ± .036
	LARGE	1.275 ± .055	1.802 ± .078	1.738 ± .027
	EVEN	1.394 ± .063	1.972 ± .089	1.691 ± .032
	ODD	1.464 ± .050	2.070 ± .071	1.921 ± .030

$$F(Z) = 4\pi \int f(\eta_i)\, f(\eta_j) \times \delta\{Z-(\eta_i\eta_j+\sqrt{1-\eta_i^2}\sqrt{1-\eta_j^2}\cos(\Delta\phi))\} \times d\eta_i d\eta_j d(\Delta\phi). \qquad (6)$$

The obtained expression of f(η) is compared with the histogram in Fig. 3 where the curve well stands for. The experimental Z distribution is compared with F(Z). Near at Z = ±1, data exceed significantly than the curves of F(Z), especially in small case. This means that two particles are correlated with each other in cms angle and sometimes are emitted in the same direction and other in the opposite direction. This correlation seems to be explain in term of the low mass clustering which rests or moves in cms.

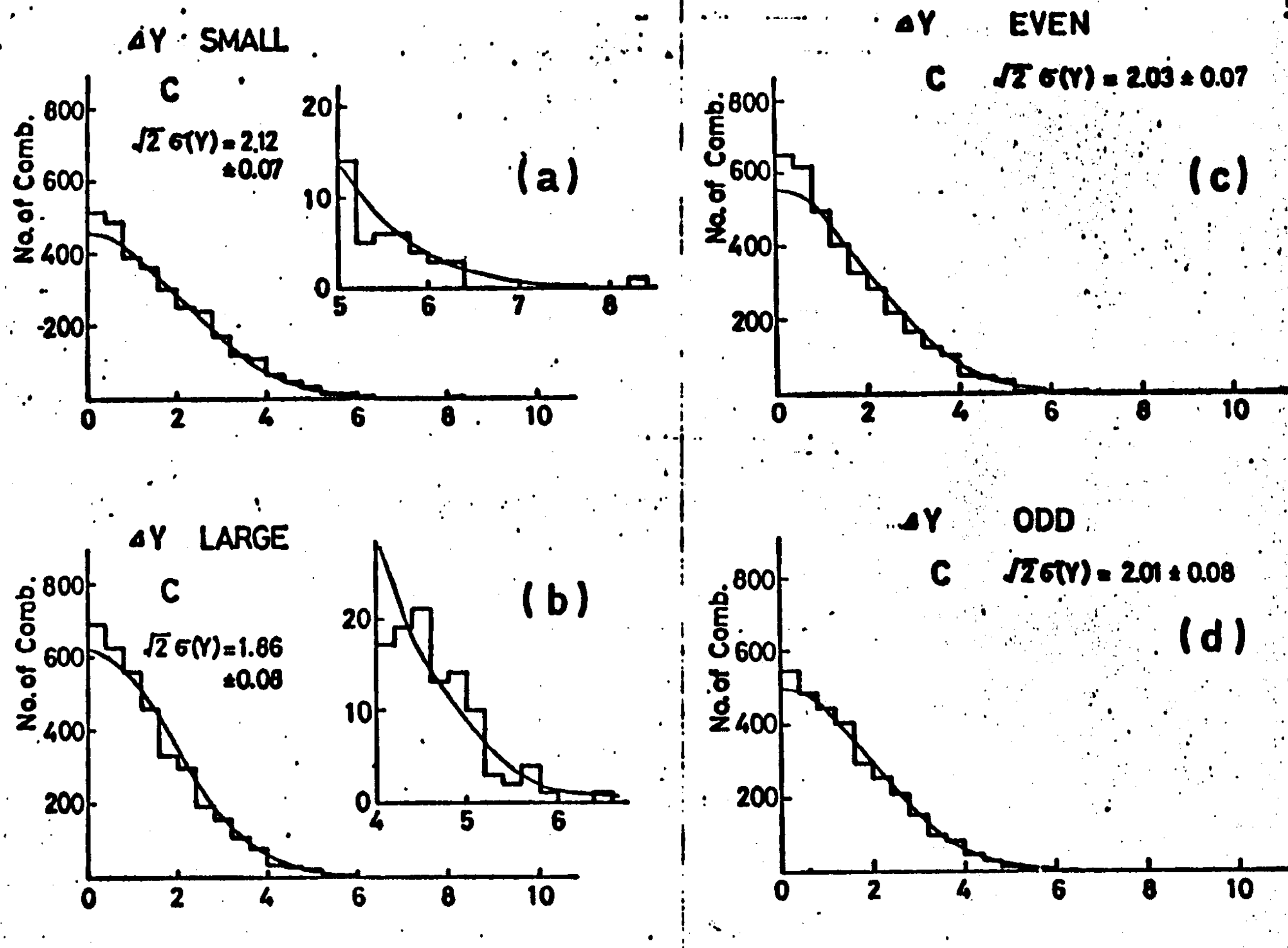

Fig. 3 Correlation of ΔY for C-events. Solid lines are Gaussian curves with $\sqrt{2}\sigma(Y)$.

6. By using the emitted angles and the azimuthal angles of the prongs in each event, we investigate the particle correlations as well as the inclusive distribution. For even and odd multiplicity events, there is no significant difference on the distributions concerned with such as Fig. 1 (c) (d), Fig. 2 (c) (d), Fig. 3 (c) and (d). The distributions for D-events are not presented here, but these are not so much different with those for clean events.

The particle correlations in ΔY and $\cos\theta^{*}_{ij}$ are found by comparing independent emission from the inclusive distributions. The correlations are remarkable for small multiplicity events.

Reference

(1) S. Konishi et al., preprint

(2) for example, J. Whitmore, Phys. Report 10C, (1974) 274.
W. T. Ko, paper presented at the XVIIth International Conference on High Energy Physics, London (1974)

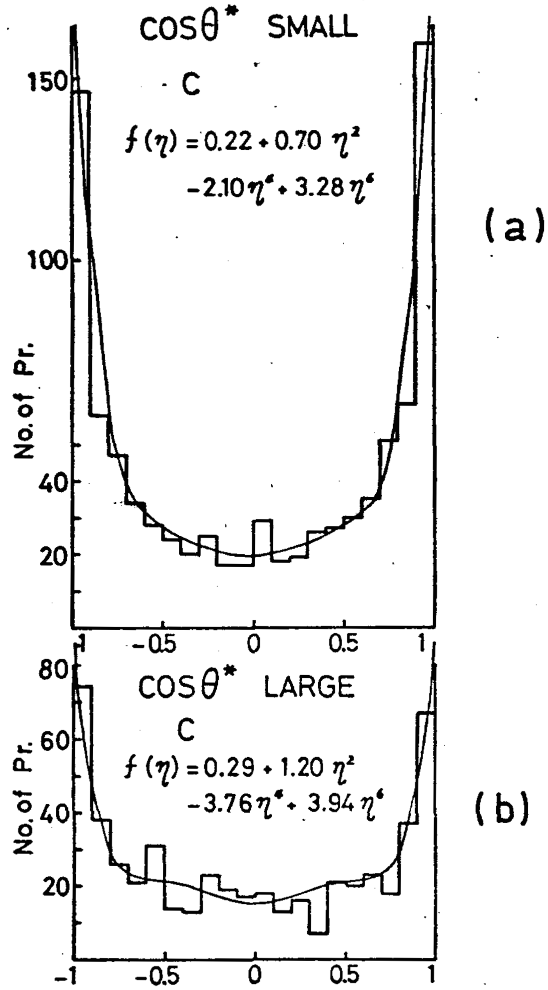

Fig. 4 Inclusive distribution of cos θ^* for small and large multiplicities of C-events. The solid curve represents the experimental formula.

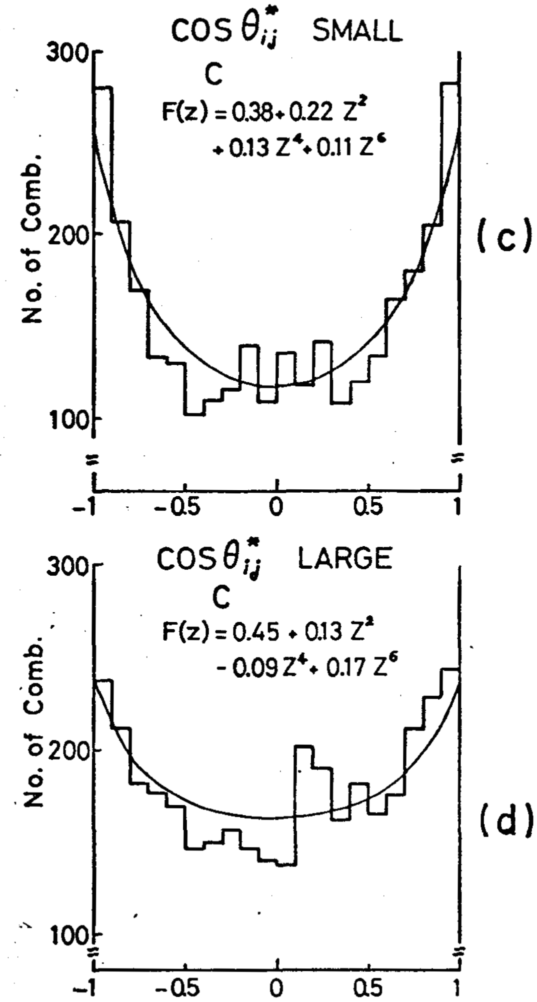

Fig. 5 Correlation of cos θ^*_{ij}. The solid curve comes from the independent emission with the inclusive distribution.